

Liquid-Metal-Elastomer Foam for Moldable Multi-Functional Triboelectric Energy Harvesting and Force Sensing

Suryakanta Nayak^{1}, Yida Li¹, Willie Tay³, Evgeny Zamburg¹, Devendra Singh¹, Chengkuo Lee¹, Soo Jin Adrian Koh², Patrick Chia³, Aaron Voon-Yew Thean^{1*}*

¹Department of Electrical and Computer Engineering, National University of Singapore, 4 Engineering Drive 3, Singapore 117583

²Department of Mechanical Engineering, National University of Singapore, 9 Engineering Drive 1, Singapore 117575

³NUS School of Design & Environment, National University of Singapore, 4 Architecture Drive, Singapore 117566

*Email: suryakanta.nayak@nus.edu.sg / suryakanta.iitkgp@gmail.com, aaron.thean@nus.edu.sg

Experimental section

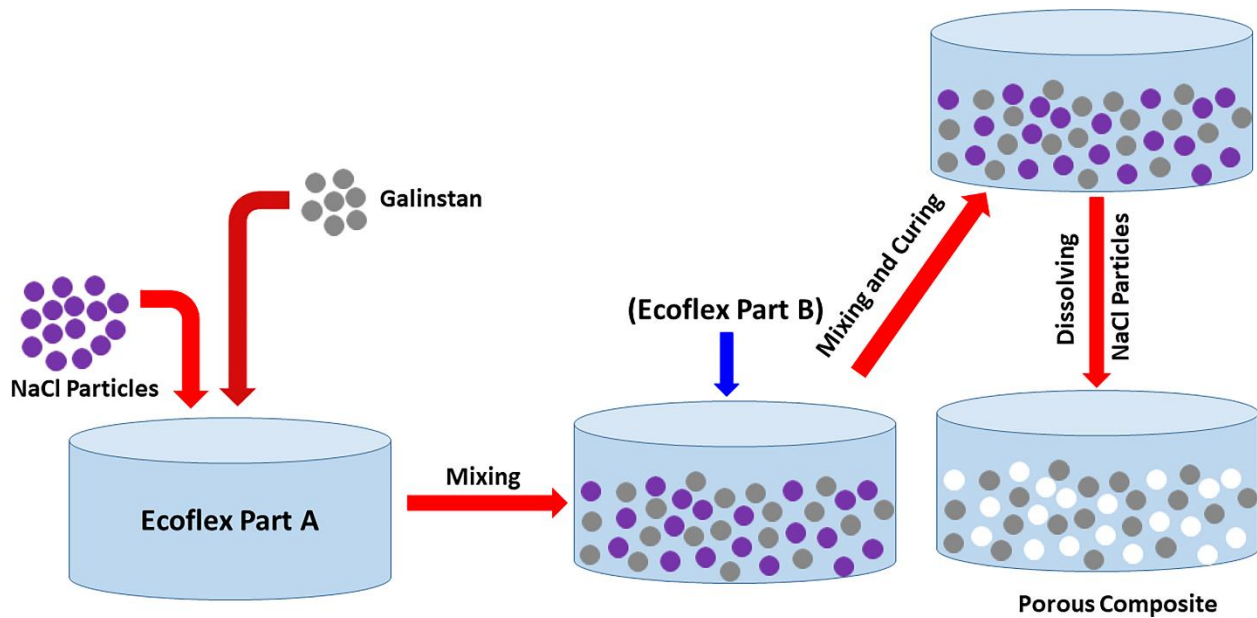
Preparation of porous LMA-Ecoflex composites

The mixing of Ecoflex (Ecoflex 0030 Part A/B, Smooth on) and other ingredients [NaCl particles (Sigma Aldrich) and liquid-metal-alloy (LMA-Galinstan, Ga₆₂In₂₂Sn₁₆, Good fellow, UK)] was done by a high-speed blender with a micro-container. In the beginning, the micro-container was kept inside a refrigerator for 15 minutes to avoid excess heating during the ingredients mixing/blending process. Then, Ecoflex 0030 (Part A) was taken in the micro-container followed by the addition of anhydrous sodium chloride particles and LMA. The mixing was done for 4 minutes at 10, 000 rpm and the above mixed mass with the container was kept inside refrigerator for 15 minutes to cool down to the room temperature. Finally, equal weight part of Ecoflex 0030 (Part B) [Part A:Part B = 1:1] was added to the above mixture and mixed for another 1.5 minutes at 10, 000 rpm. The above composite mixtures were casted into different acrylic molds and cured at 90 °C for 30 minutes. The cured composites were immersed in hot deionized (DI) water (heated at 250 °C) for 1 h followed by 24 h in cold water and this step was repeated three times. Fresh DI water was used after every 24 h to ensure that all the salt dissolved completely. After the above process, the samples with DI water were kept in furnace at 90 °C for 72 h, where fresh DI water was used after every 24 h. Here, NaCl salt was used as a sacrificial template. The mass ratio between the NaCl powder and Ecoflex in LMA-Ecoflex composites was adjusted to control the porosity. The porosity of the samples was calculated by the equation given below.^[1, 2]

$$\left(1 - \frac{M_0}{M}\right) \times 100 \% \dots\dots\dots(1)$$

Where, M_0 and M are the mass of porous and the solid samples that with the same volume as the porous one, respectively.

The schematic for the preparation of porous LMA-Ecoflex composites is shown in **Scheme S1**. In all the composites, 10 g (parts) of Ecoflex is used as the base matrix. The concentration (by weight parts) of LMA and NaCl is varied with respect to the above base matrix (Ecoflex). The detailed compositions of all composites are given in **Table S1**.



Scheme S1 Schematic presentation for the preparation of porous LMA-Ecoflex composites.

Table S1 Formulations of porous LMA-Ecoflex (LE) composites (NaCl and LMA are varied by weight part with respect to 10 parts of Ecoflex).

| Composite | Ecoflex 0030 (Part A:B = 1:1) (gm) | NaCl (gm, by part) | LMA (gm, by part) |
|-----------|------------------------------------------|--------------------------|-------------------------|
| LE-1 | 10 | 5 | 1 |
| LE-2 | 10 | 5 | 2 |
| LE-3 | 10 | 5 | 3 |

| | | | |
|------|----|---|---|
| LE-4 | 10 | 5 | 4 |
| LE-5 | 10 | 5 | 5 |
| LE-6 | 10 | 5 | 7 |
| LE-7 | 10 | 5 | 9 |
| LE-8 | 10 | 7 | 3 |
| LE-9 | 10 | 9 | 3 |

* L = Liquid metal alloy (LMA); E = Ecoflex

Fig. S1 shows the photographs of LMA-Ecoflex composites before (**Fig. S1a**) and after NaCl removal (**Fig. S1b, S1c**). The sample surface before salt removal was smooth (**Fig. S1a**), which becomes little rough after salt removal. Samples with different shape and sizes were prepared by different type of molds (circular/rectangular). So, the above composites can be molded into any kind of 3D-structures. The flexibility of the composite can be seen from the cross-sectional image (**Fig. S1c**). **Fig. S2a** shows the 2D surface profiling image of LMA-Ecoflex composite [3 weight parts of LMA in Ecoflex matrix (LMA:NaCl:Ecoflex = 3:5:10)] taken by optical microscope, where the size and depth of cavities are clearly observed (**Fig. S2b**). The size of the pores is in the ranges of 100-500 μm and depth of $\sim 500 \mu\text{m}$ (maximum) as seen from **Fig. S2b**.

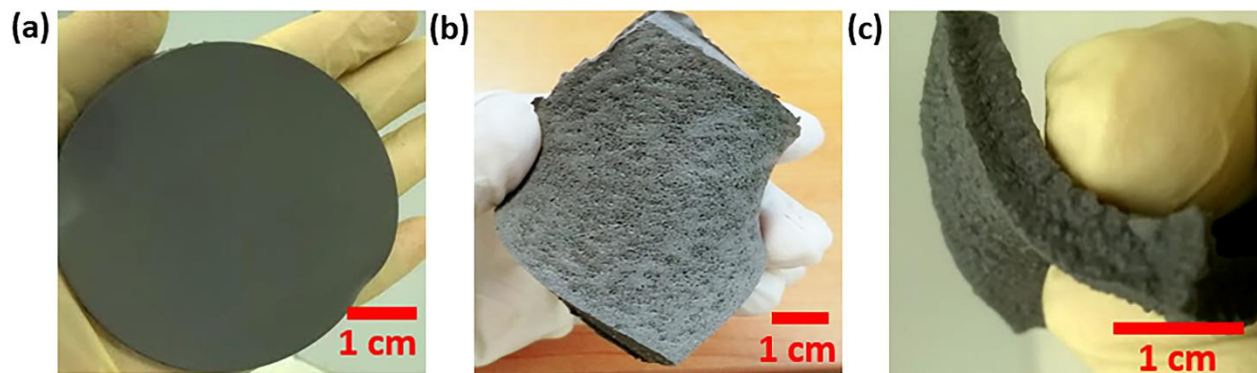


Fig. S1 (a) Photograph of an as-prepared LMA-Ecoflex composite, (b) photograph of the porous composite foam after dissolving salt (pores seen in naked eye), (c) photograph of the cross-sectional view of LMA-Ecoflex composite foam.

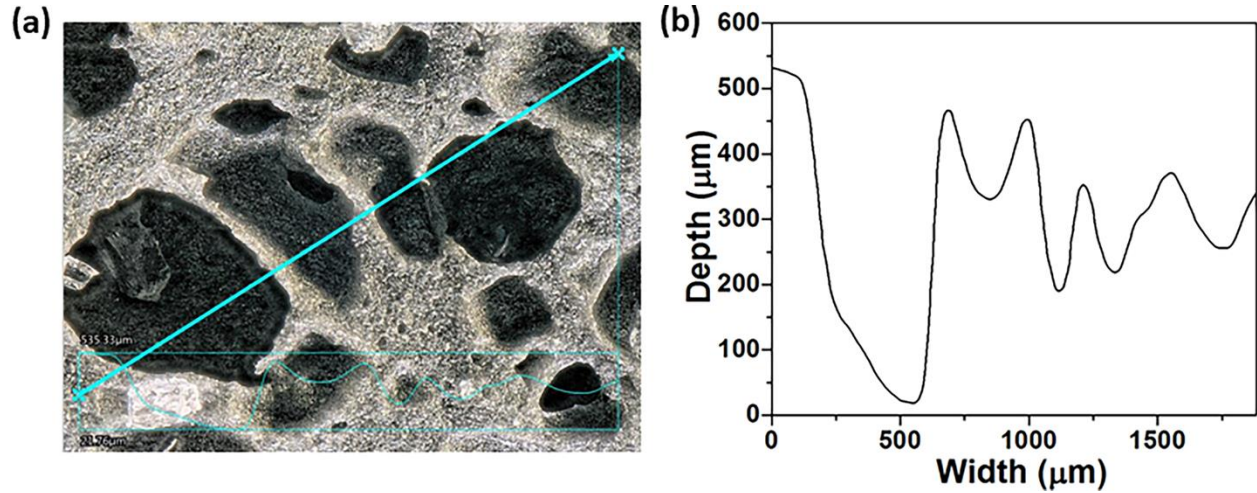


Fig. S2 (a, b) Surface profiling of porous composite (LE-3) by microscope.

Measurements and characterization:

The composite mixtures were prepared by high speed blender (MX1300XTXEE, Waring) and micro-container (Eberbach E8575, Waring). The output open-circuit voltage (V_{OC}) and short-circuit current (I_{SC}) was measured by B2902A Precision Source/Measure Unit. The cyclic compressive force was given by a mechanical tester (Multitest 2.5-i). Morphology of the composites was studied through scanning electron microscope (Philips SEM XL-30) and optical microscope (Keyence microscope, VHX 5000). Electrostatic force microscopy (EFM) images were taken by Dimension Icon ScanAsyst, Bruker to understand the electricity generation mechanism. Mechanical tests were done by the universal testing machine (Zwick/Roell Z2.5). The AC conductivity/resistivity of the porous nanocomposites was studied by Navocontrol dielectric spectrometer (Navocontrol Alpha A spectrometer). The change in capacitance with

loading/unloading was studied by an LCZ meter (2321, NF Electronic Instruments) with its test fixture (2323A, NF Electronic Instruments).

Scanning electron microscopy (SEM)

The SEM images of LMA-Ecoflex composite [3 weight parts of LMA in Ecoflex (LMA:NaCl:Ecoflex = 3:5:10)] is shown in **Fig. S3** and their respective elemental composition values are given in **Table S2**. It is observed that there is minor quantity of NaCl particles in the composite as seen from **Table S2 (Fig. S3b and S3d)**. To confirm the presence of NaCl crystal, EDX spectrum was taken, which is presented in **Fig. S3c**. It is observed from **Table S2 (Fig. S3c)** that the concentration of “Na” / “Cl” atom is more, where concentration of other elements is either zero (In/Sn) or negligible, which confirms the presence of some NaCl crystal. The presence of Ga, In, and Sn (from Galinstan, $\text{Ga}_{62}\text{In}_{22}\text{Sn}_{16}$) in the composite is confirmed by EDX measurement of the composite as shown in **Fig. S3a** and **Table S2**. The uniform dispersion and distribution of LMA in the above porous composites is also confirmed from the EDX data (**Table S2 data for Fig. S3b and S3d**), where there is minor variation in concentration of Ga, In, and Sn at different locations of the composites. The composite was coated with “Au” by sputtering process to make its surface conductive and to avoid surface charging during SEM measurement. So, there is presence of “Au” in EDX spectrum as reported in **Table S2**.

Table S2 SEM-EDX data (obtained from Fig. S3) for porous composite (LE-3).

| For Figures 4a | | | For Figures 4b | | | For Figure Fig. 4c | | | For Figure 4d | | |
|----------------|-------|-------|----------------|--------|--------|--------------------|--------|--------|---------------|--------|--------|
| Element | Wt % | At % | Element | Wt % | At % | Element | Wt % | At % | Element | Wt % | At % |
| GaL | 68.35 | 78.30 | O K | 14.13 | 31.99 | O K | 3.08 | 7.02 | O K | 14.89 | 32.32 |
| InL | 17.72 | 12.32 | SiK | 44.92 | 57.92 | SiK | 0.47 | 0.60 | SiK | 47.33 | 58.51 |
| SnL | 13.93 | 9.38 | GaL | 0.94 | 0.49 | GaL | 4.17 | 2.18 | GaL | 1.00 | 0.50 |
| Total | 100 | 100 | InL | 0.53 | 0.17 | InL | 0.00 | 0.00 | InL | 0.55 | 0.17 |
| | | | SnL | 0.58 | 0.18 | SnL | 0.00 | 0.00 | SnL | 0.60 | 0.18 |
| | | | NaK | 0.91 | 1.44 | NaK | 22.77 | 36.04 | NaK | 0.96 | 1.46 |
| | | | ClK | 1.02 | 1.05 | ClK | 49.16 | 50.47 | ClK | 1.08 | 1.06 |
| | | | AuM | 36.97 | 6.76 | AuM | 20.36 | 3.69 | AuM | 33.58 | 5.81 |
| | | | Total | 100.00 | 100.00 | Total | 100.00 | 100.00 | Total | 100.00 | 100.00 |

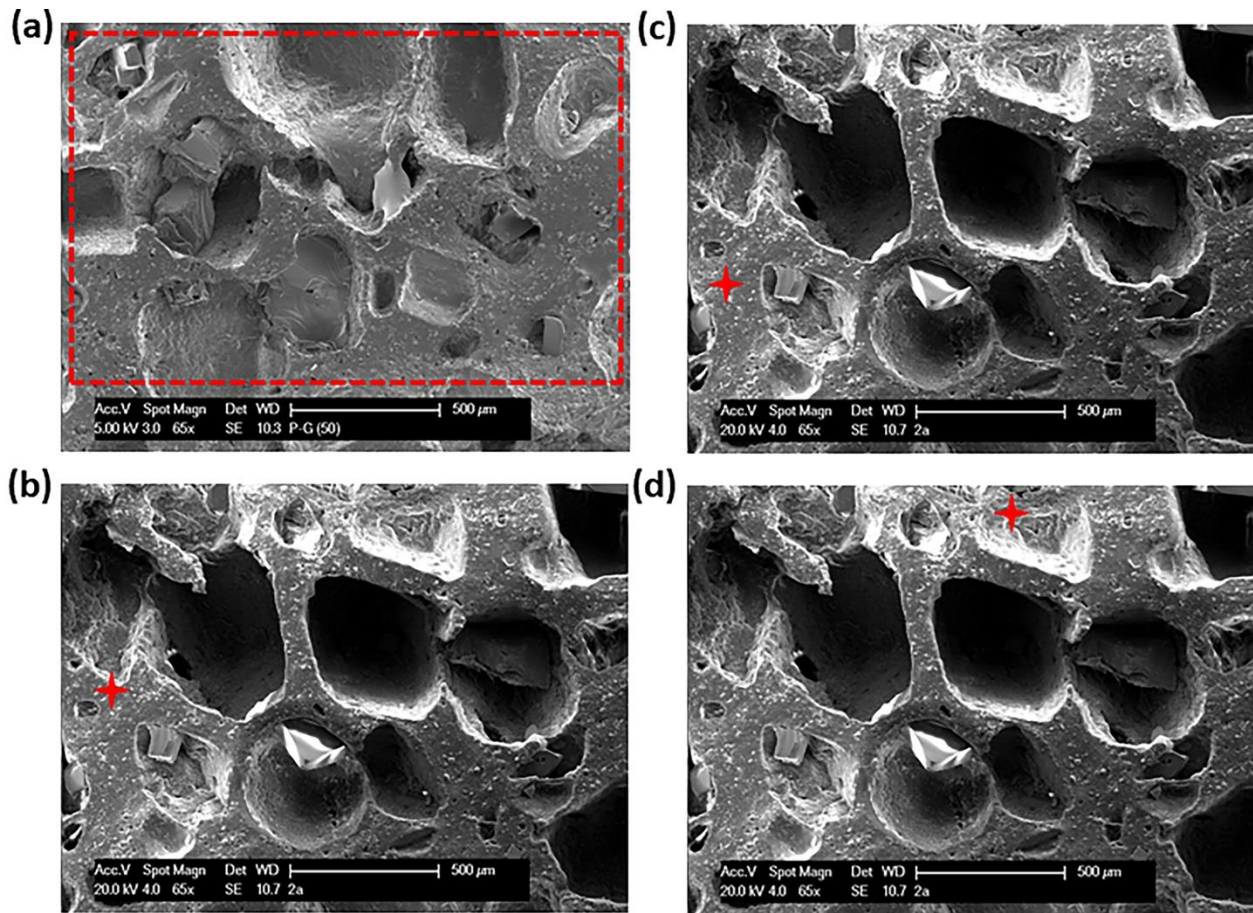


Fig. S3 SEM images of porous composite containing 3 weight parts of LMA in 10 parts of Ecoflex (LMA:NaCl:Ecoflex = 3:5:10).

Influence of LMA loading on triboelectric output

All composites of different concentration of LMA are studied with respect to compression up to certain depth (**Scheme S2**). In compression mode, both top and bottom electrodes were in continuous contact with the composite during compressive cycles. The output short circuit current (I_{SC}) and open circuit voltage (V_{OC}) are measured with respect to deformation cycles for different samples. **Fig. S4** shows the output current (I_{SC}) and voltage (V_{OC}) upon 5 mm depth compressible cycles. We observed that the foam generates the largest electrical output at 3 weight parts of LMA in Ecoflex matrix composite (LMA:NaCl:Ecoflex = 3:5:10), producing a

peak-to-peak output current (I_{SC}) of ~ 466 nA (charge density = ~ 35 $\mu\text{C}/\text{m}^2$, **Fig. S4a**) and peak voltage (V_{OC}) of ~ 78 V (**Fig. S4b**) for a sample of dimension 5 cm x 5 cm x 1 cm, where the output current is ~ 20 % higher than previously reported triboelectric foams based on PDMS and PZT/CNT of equivalent area.^[1,2]

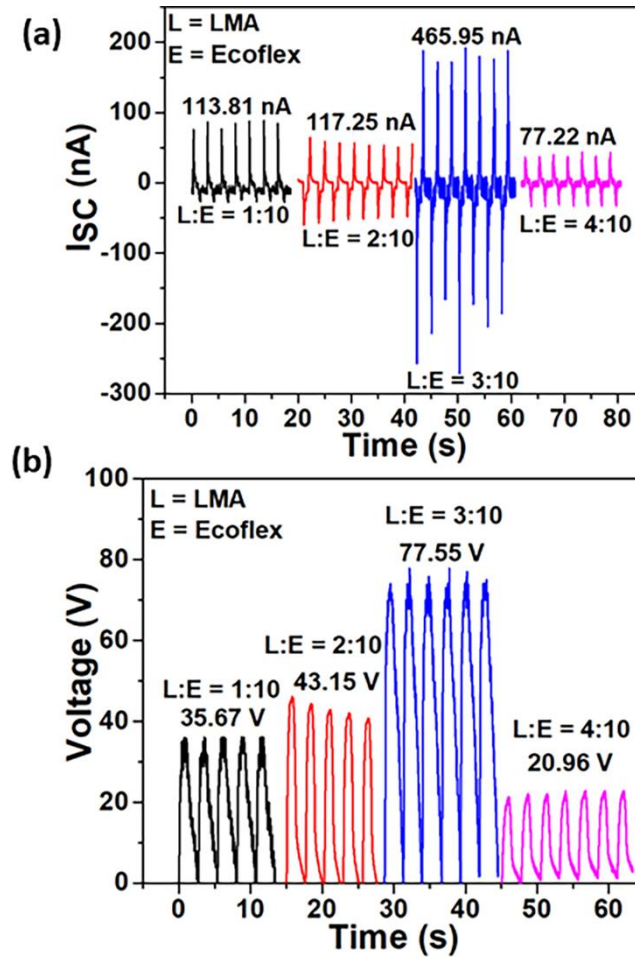


Fig. S4 Peak-to-peak (a) current and (b) voltage for porous LMA-Ecoflex composites with different loadings of LMA under 5 mm depth compressive cycles and at an operation frequency of ~ 0.4 Hz (**Scheme S2**) [Sample dimension: 5 cm x 5 cm x 1 cm]. All composites were prepared with 5 weight parts of NaCl particles.

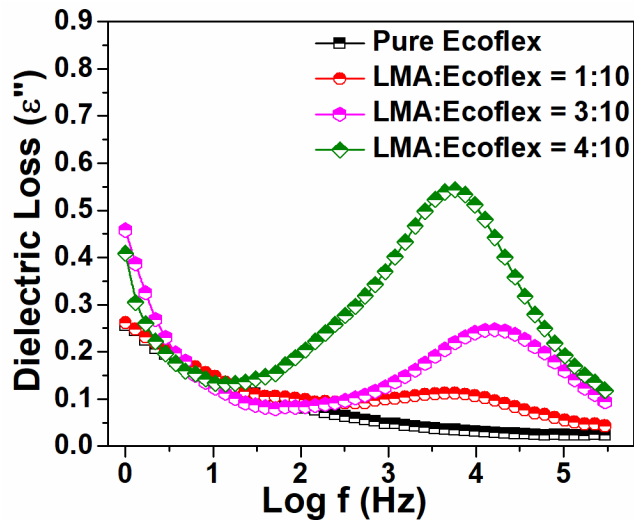


Fig. S5 Frequency dependent dielectric loss of LMA-Ecoflex composites with varying LMA concentrations. All composites were prepared with 5 weight parts of NaCl particles.

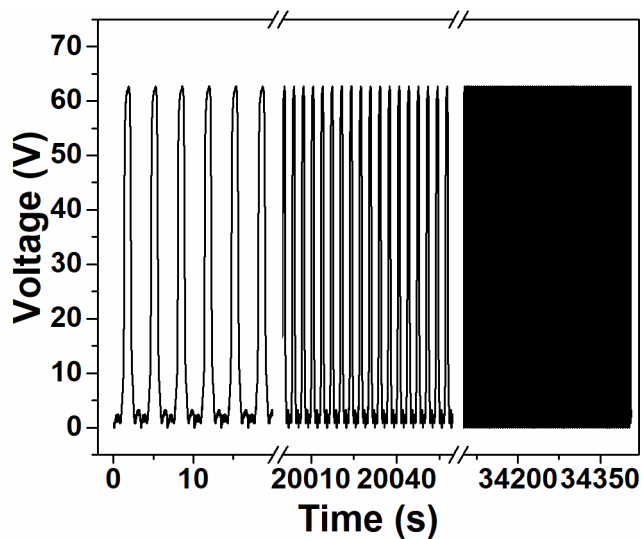


Fig. S6 The stability of the Ecoflex-LMA TENG (LMA:NaCl:Ecoflex = 3:5:10), where voltage (V_{OC}) was measured for more than 10, 000 compressible cycles (at compression depth = 5 mm) at an operation frequency of ~ 0.4 Hz.

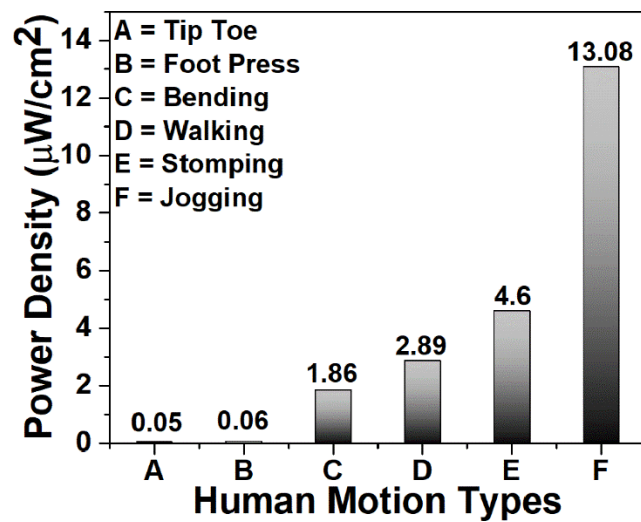


Fig. S7 Variation of power density with different human motion types (using the shoe insole).

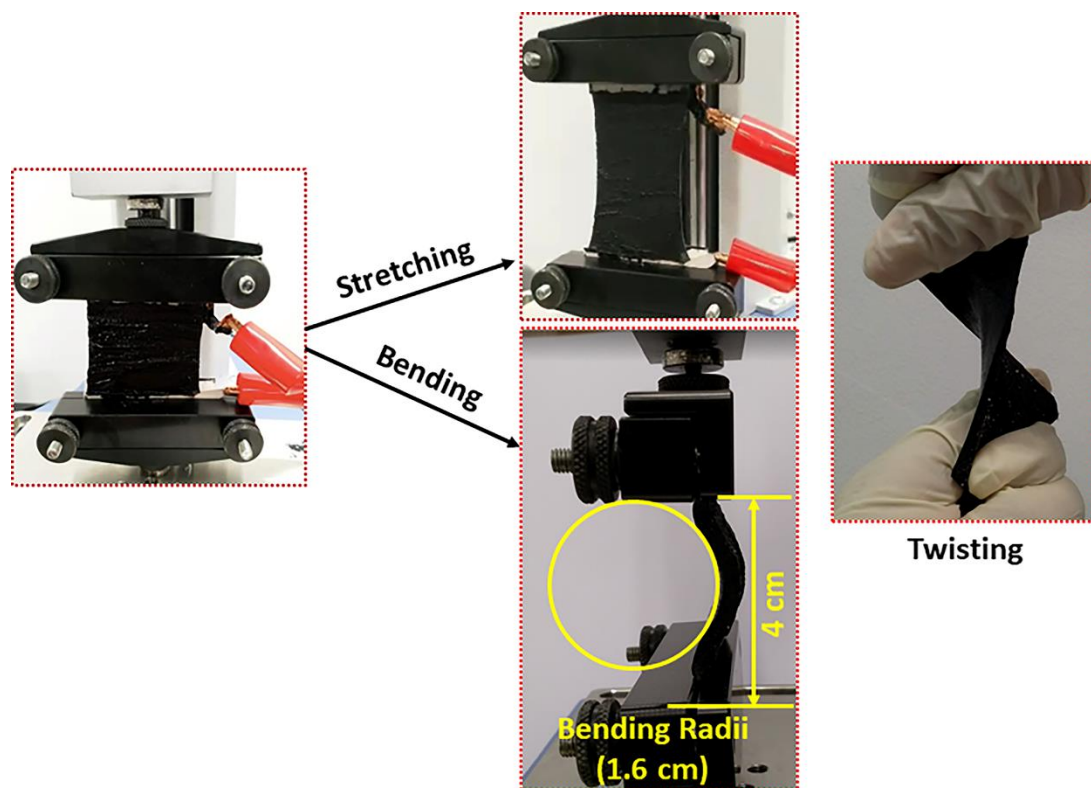


Fig. S8 Stretching, bending, and twisting of a sample of dimension 5 cm x 5 cm x 0.2 cm.

28

Mechanical properties

The variation of Young's modulus with LMA loading in Ecoflex matrix is presented in **Fig. S9**. The measurement was done on composites before and after NaCl removal. The Young's modulus of pure Ecoflex is 41 kPa at 100 % strain. There is increase in modulus with increase in LMA concentration, but the increase up to a certain LMA concentration (LMA:Ecoflex = 5:10) for composites before NaCl removal. The increase in modulus with LMA loading is due its incompressible behavior. However, after 5 weight parts by weight of LMA loading in 10 part of Ecoflex composite (LMA:NaCl:Ecoflex = 5:5:10), there is decrease in modulus which may be due the flow behavior of LMA at high loading. There is decrease in modulus when the salt

particles removed, and the matrix become porous. It confirms that the matrix become softer when it became porous.

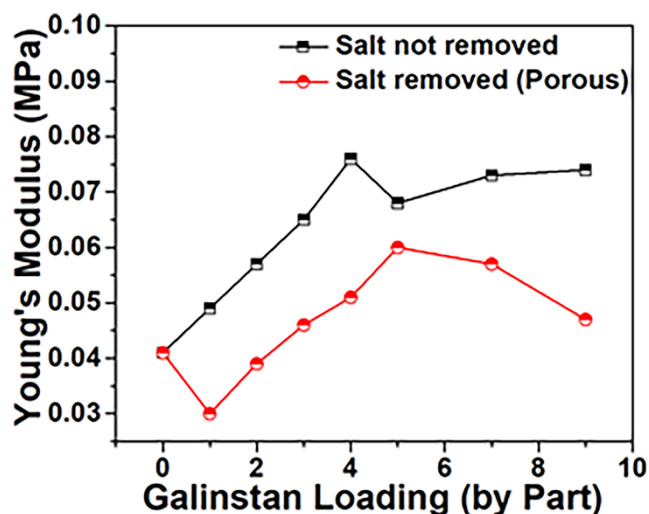


Fig. S9 Variation of Young's modulus with LMA loading for both porous and non-porous composites. All composites were prepared with 5 weight parts of NaCl particles.

We have conducted high frequency test manually due to the speed limitation of our equipment (1 Hz, mechanical tester, Multitest 2.5-i) to see the difference in current output (contact-separation). At higher frequency (~2.5 Hz) the maximum output current is almost 6 times (1.2 μ A_ Fig. S10) more than which measured at ~0.4 Hz (212 nA, Fig. 6a).

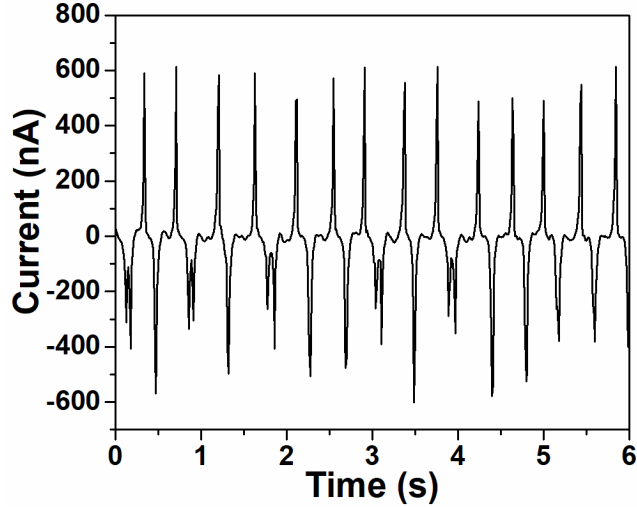


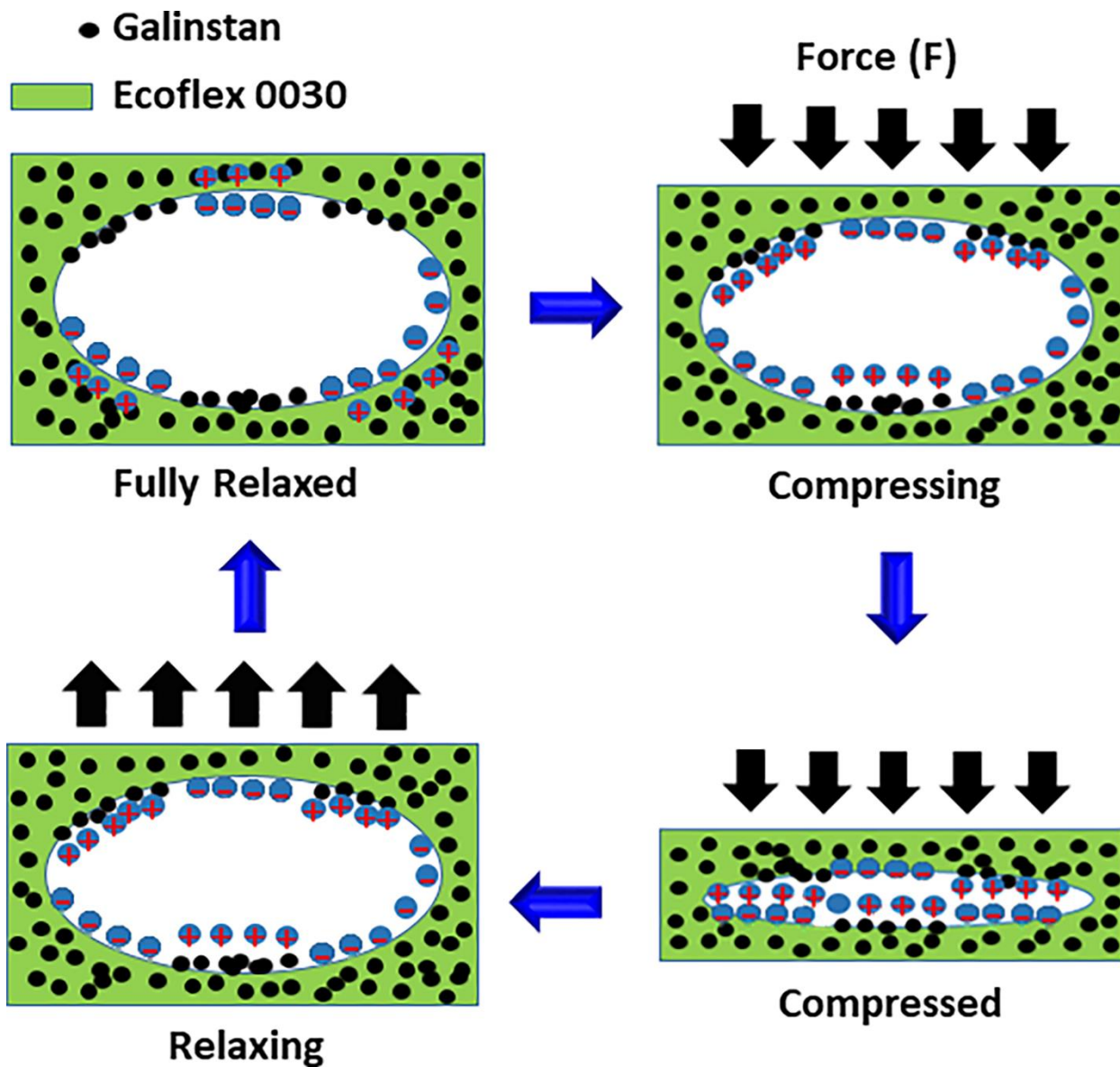
Fig. S10 Effect of high operation frequency (~2.5 Hz) on the output current for the porous composite containing 3 weight parts of LMA (LMA:NaCl:Ecoflex = 3:5:10) in case of contact-separation mode.

Charge generation mechanism

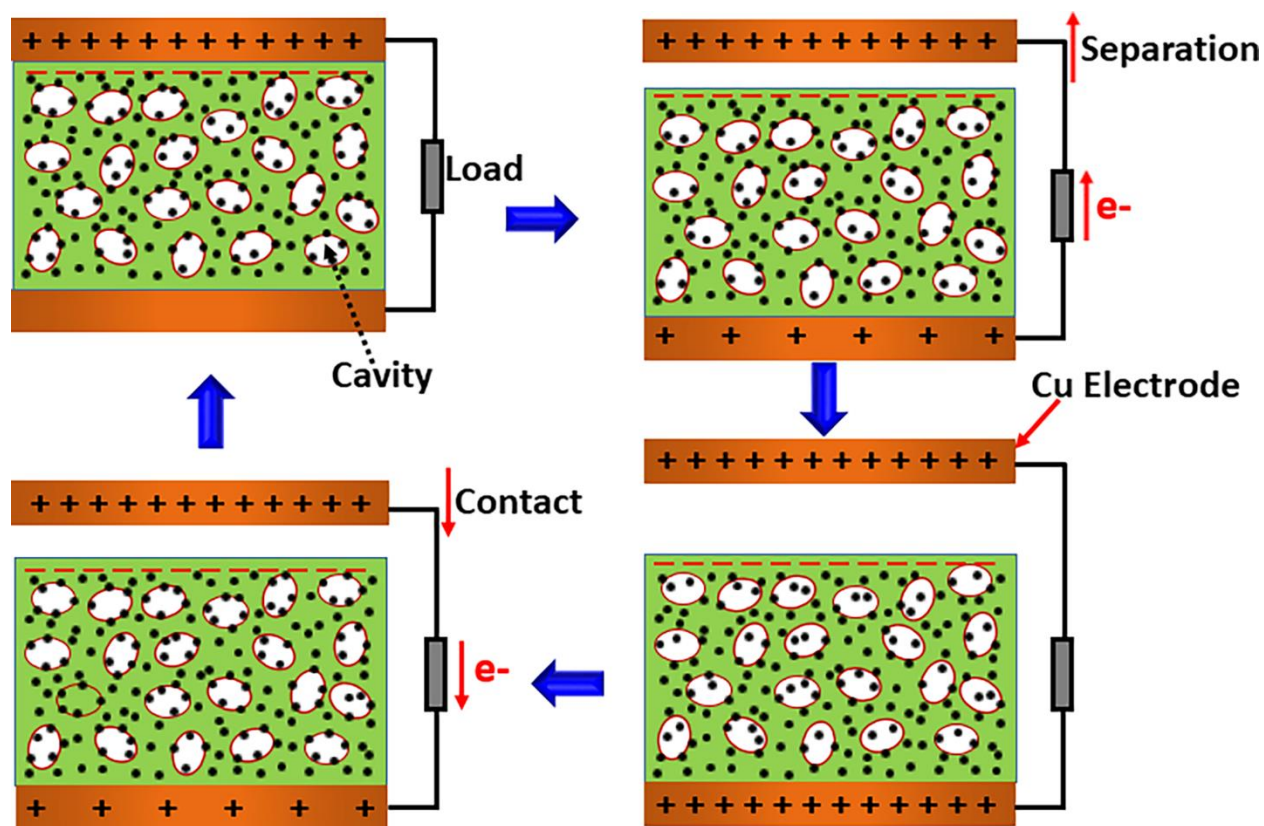
From dielectric measurement, we have observed that the porous LMA-Ecoflex composites are insulating in nature when LMA concentrations are optimized to maximize triboelectric charge generation (Fig. 3d and Fig. S5 in SI). Under low leakage (loss) conditions, the triboelectric charges are largely localized in the composite matrix with no charge flow. We have shown that the charges are mirrored capacitively (i.e. image charge) to the electrodes, upon generation. This observation is supported by the increase in current/charge generation with increasing dielectric constant of the composite (due to increase in LMA concentration), consistent with capacitance increase (Fig. 3d). The composites with large number of cavities forms complex capacitors structure as these tiny cavities behaves as micro-capacitors. Although the specific mechanism for the complex pore network is not fully described, we identified the origin of the charge to be the pores plus LMA, and likely due to contact-separation like mode at the pore level. We expect its

mechanism somewhat similar to contact-separation triboelectric mode as there contact-separation happens due to compression-relaxation cycles. Due to compression-relaxation process, contact-separation happens between top and bottom walls of the cavities that produce negative charges on insulating Ecoflex surface due to its more electronegative behavior as per triboelectric series and leaves positive charges on region with high concentration of conducting LMA.^[2] With repeated cycles, more and more charges generated at the pores and transported to the electrode in capacitive manner as discussed above. As electrodes are placed on top and bottom of the porous composites, these positive-negative charge separation produces an open-circuit potential difference (V_{OC}) that leads to a short-circuit current (I_{SC}). As the pore undergoes the relaxation, the I_{SC} reverses. **Scheme S2** shows a single pore structure which shows that negative charges are gained by the Ecoflex surface and leaves positive charge on the region with more LMA.

We proposed a detailed mechanism for the contact-separation mode happened between top electrode and the porous composite. Initially, when the top electrode touches the composite surface it produces negative charges on the composite surface and leaves positive charge on the top electrode. When the two surfaces separated by a small gap, a potential drop is created. As both electrodes are connected by a load, free electrons from bottom electrode would flow to the top electrode to build an opposite potential in order to balance the electrostatic field. Again, when the gap is closed, the triboelectric charges created potential disappears and electrons flows back from top electrode to the bottom electrode (**Scheme S3**).^[3]



Scheme S2 Schematic representation of energy harvesting mechanism involved during compression-relaxation cycles of a single cavity.



Scheme S3 Schematic representation of energy harvesting mechanism involved during contact-separation between top copper electrode and the porous composite (also see Fig. 5a).

Table S3 Output performance comparison of nanogenerators.

| S. No. | Nanogenerators | Instantaneous Power Density ($\mu\text{W}/\text{cm}^2$) | Current | Voltage (V) | Power (mW) | Reference |
|--------|--------------------------------------------------------|-----------------------------------------------------------|-------------------------|-------------|-------------------|---------------------|
| 1 | PDMS-PZT (Porous) | 0.4 | 116 nA | 29 | 0.003 | [1] |
| 2 | PDMS-CNT (Porous) | ~0.7 (Calculated from Fig. 4) | 180 nA | 60 | 0.009 | [2] |
| 3 | PDMS/BaTiO ₃ /carbon nanotubes (Non-porous) | *** | 250 nA | 3.2 | 0.0008 | [4] |
| 4 | PDMS/PZT/Ag nanowires (Non-porous) | *** | 130 nA | 1.7 | 0.0002 | [5] |
| 5 | PDMS/BaTiO ₃ (Non-porous) | *** | 350 nA | 5.5 | 0.0019 | [6] |
| 6 | Fe-RGO/PVDF (Non-porous) | *** | 254 nA | 5.1 | 0.0012 | [7] |
| 7 | Hybrid nanofibers/carbon electrode (Non-porous) | *** | 189 nA | 9.3 | 0.0017 | [8] |
| 8 | ECOFLEX-Galinstan (Porous) | 1.44 (Flat Sample); 13 (Shoe Insole) | 233 nA | 78 | 0.02 | Present Work |
| | | | | | Flat Sample _5 cm | |
| | | | Flat Sample_5 cm x 5 cm | | x 5 cm | |
| | | | 12.81 μA | 199.25 | 2.6 | |
| | | | Shoe Insole | | Shoe Insole | |

In **Table S3**, we have compared the output performance of our nanogenerator with previous works. Our samples are porous Ecoflex-Galinstan composite, and the output current/voltage generation purely depends on the compression-relaxation mode. If we compare the output performance, present work is better compared to previously reported works.

References

- [1] Ma SW, Fan YJ, Li HY, Su L, Wang ZL, Zhu G. ACS Appl Mater Interfaces 2018;10:33105.
- [2] Fan YJ, Meng XS, Li HY, Kuang SY, Zhang L, Wu Y, Wang ZL, Zhu G. Advanced Materials 2017;29:1603115 (1).
- [3] Wang ZL. Faraday Discussions 2014;176:447.
- [4] Park KI, Lee M, Liu Y, Moon S, Hwang GT, Zhu G, Kim JE, Kim SO, Kim DK, Wang ZL. Advanced Materials 2012;24:2999.
- [5] Jung WS, Lee MJ, Yoon SJ, Lee WH, Ju BK, Kang CY. International Journal of Applied Ceramic Technology 2016;13:480.
- [6] Lin Z-H, Yang Y, Wu JM, Liu Y, Zhang F, Wang ZL. The journal of physical chemistry letters 2012;3:3599.
- [7] Karan SK, Mandal D, Khatua BB. Nanoscale 2015;7:10655.
- [8] Siddiqui S, Lee HB, Kim DI, Duy LT, Hanif A, Lee NE. Advanced Energy Materials 2018;8:1701520 (1).